Inorg. Chem. **2004**, *43*, 6936–6943

Binding of Inorganic Oxoanions to Macrocyclic Ligands: Effect of the Degree of Protonation on Supramolecular Assemblies Formed by Phosphate and [18]aneN$_6$

Andrew C. Warden, Mark Warren, Milton T. W. Hearn,† and Leone Spiccia*

School of Chemistry, Monash University, Victoria, 3800, Australia, and
Center for Green Chemistry, School of Chemistry, Monash University, Victoria, 3800, Australia

Received March 19, 2004

Five macrocycle-oxoanion adducts have been isolated from aqueous solutions containing 1,4,7,10,13,16-hexaazacyclooctadecane ([18]aneN$_6$, **L**) and phosphoric acid whose pH had been adjusted to selected values in the 1–8 range. Four products, (H$_6$**L**)(H$_2$PO$_4$)$_6$·2H$_3$PO$_4$ (**1**), (H$_6$**L**)(H$_2$PO$_4$)$_6$ (**2**), (H$_4$**L**)(H$_2$PO$_4$)$_4$·2H$_2$O (**4**), and (H$_4$**L**)(HPO$_4$)$_2$·7H$_2$O (**5**) crystallized from aqueous solutions at pH 1, 3, 6, and 8, respectively, while (H$_4$**L**)(H$_2$PO$_4$)$_4$ (**3**) crystallized on diffusion of EtOH into an aqueous reaction mixture at pH 6. Single-crystal X-ray structure determinations enabled an examination of supramolecular interactions between protonated forms of [18]aneN$_6$, phosphoric acid and its conjugate bases, and water of solvation. The macrocycle adopts a variety of conformations in order to accommodate the supramolecular constructs formed by the oxoanions and solvent molecules as the relative proportions of interacting species are altered. At pH 1 and 3, the fully protonated macrocycle, [LH$_6$]$^{6+}$, is found with six $H_2PO_4^-$ anions. At pH 6 and 8, the tetraprotonated macrocycle, [LH$_4$]$^{4+}$, crystallizes with four $H_2PO_4^-$ and two HPO_4^{2-}, respectively. Variations in the solute of crystallization are evident, with phosphoric acid being present at the lowest pH and water at pH 6 and 8. In **5**, the seven unique water molecules form a string-of-pearls motif within which a new heptameric isomer, consisting of a water pentamer that uses a single water to interact with the other two unique water molecules, is found. Structures **1**, **2**, **4**, and **5** exhibit η-3 H-bonding of ammonium protons to a single oxygen of the guest phosphates located above and below the macrocyclic ring. In **3**, two phosphate oxygens of the cavity anion interact with the macrocycle, one of which participates in η-2 H-bonding with ammonium groups.

Introduction

The supramolecular chemistry of anions plays a vast and many-faceted role in both biological and inorganic systems.[1] A survey of 67 protein structures has identified a structural feature known as "The Nest" that has the potential to bind to anions and to partially negatively charged groups (e.g., carbonyls from peptide backbones) via supramolecular interactions that can involve main-chain NH groups.[2] Polyammonium macrocycles,[3−10] cyclic amides,[11] and cyclic peptides[12] have been reported as hosts for anions, as have metal complexes of polyoxo-[13] and polyaza-macrocycles.[14−17] Su-

* Author to whom correspondence should be addressed. E-mail: leone.spiccia@sci.monash.edu.au.
† Center for Green Chemistry.

(1) (a) *Supramolecular Chemistry of Anions*; Bianci, A.; Bowman-James, K.; Garcia-España, E., Eds.; Wiley-VCH: New York, 1997 and references therein. (b) Beer, P. D.; Wheeler, J. W.; Moore, C. In *Supramolecular Chemistry*; Balzani, V.; De Cola, L., Eds.; Kluwer Academic Publishers: Dordrecht, 1992 and references therein.
(2) Watson, J. D.; James Milner-White, E. *J. Mol. Biol.* **2002**, *315*, 171.
(3) Deitrich, B.; Hosseini, M. W.; Lehn, J. M.; Sessions, R. B. *J. Am. Chem. Soc.* **1981**, *103*, 1282.
(4) Hosseini, M. W.; Lehn, J. M. *J. Am. Chem. Soc.* **1982**, *104*, 3525.
(5) Haj-Zaroubi, M.; Mitzel, N. W.; Schmidtchen, F. P. *Angew. Chem., Int. Ed.* **2002**, *41*, 104.
(6) Bazzicalupi, C.; Bencini, A.; Bianchi, A.; Cecchi, M.; Escuder, B.; Fusi, V.; Garcia-España, E.; Giorgi, C.; Luis, S. V.; Maccagni, G.; Marcelino, V.; Paoletti, P.; Valtancoli, B. *J. Am. Chem. Soc.* **1999**, *121*, 6807.
(7) Arranz, P.; Bencini, A.; Bianchi, A.; Diaz, P.; Garcia-España, E.; Giorgi, C.; Luis, S. V.; Querol, M.; Valtancoli, B. *J. Chem. Soc., Perkin Trans. 2* **2001**, 1765.
(8) (a) Lu, Q.; Motekaitis, R. J.; Reibenspies, J. J.; Martell, A. E. *Inorg. Chem.* **1995**, *34*, 4958. (b) Martell, A. E.; Motekaitis, R. J.; Lu, Q.; Nation, D. A. *Polyhedron* **1999**, *18*, 3203.
(9) Nation, D. A.; Reibenspies, J.; Martell, A. E. *Inorg. Chem.* **1996**, *35*, 4597.
(10) Pina, F.; Parola, A. J. *Coord. Chem. Rev.* **1999**, *185−186*, 149.
(11) (a) Choi, K.; Hamilton, A. D. *J. Am. Chem. Soc.* **2001**, *123*, 2456. (b) Hossain, A.; Llinares, J. M.; Powell, D.; Bowman-James, K. *J. Am. Chem. Soc.* **2001**, *40*, 2936. (c) Piatek, P.; Jurczak, J. *Chem. Commun.* **2002**, 2450.
(12) Kubik, S.; Goddard, R. *Proc. Nat. Acad. Sci.* **2002**, *99*, 5127.

10.1021/ic049633v CCC: $27.50
Published on Web 10/01/2004

pramolecular interactions are being exploited in the development of, for example, chemosensors for inorganic phosphates based on colorimetry,[18] fluorescence,[19] electrochemistry, and potentiometry.[8b]

Inorganic oxoanions, and in particular pyrophosphates and phosphates, have been studied as guests in a variety of host−guest complexes[1,6,19,20] owing to their biological and environmental significance. The ability of these anions to form supramolecular assemblies with polyammonium macrocycles, held together by electrostatic and H-bonding interactions, has heightened interest in host−guest complementarity. From a biological perspective, polyammonium macrocycles comprise a remarkably versatile family of phosphate hosts that can also bind ADP and ATP.[20−22] Bazzicalupi et al. have conducted detailed thermodynamic studies of pyrophosphate and phosphate binding to a series of polyammonium macrocycles,[6] including 1,4,7,10,13,16-hexaazacyclooctadecane ([18]aneN$_6$, **L**) that indicate an increase in binding affinity with increasing degree of protonation of the macrocycle. The crystal structures of two adducts formed by dihydrogen pyrophosphate and two macrocycles (**L** and 1,10-dimethyl-[18]aneN$_6$) reported in the paper[6] revealed that each tetraprotonated macrocycle interacts with two $H_2P_2O_7^{2-}$ anions, one above and one below the plane of the ring. Both structures exhibited η-3 H-bonding of the ammonium protons to one of the oxygen atoms on the anions.

We have prepared five oxoanion-macrocycle adducts consisting of two polyammonium forms of [18]aneN$_6$ {[18]-aneN$_6$H$_4$}$^{4+}$ and {[18]aneN$_6$H$_6$}$^{6+}$} and two conjugate bases of phosphoric acid, $H_2PO_4^-$ and HPO_4^{2-}. X-ray crystal structure determinations have elucidated cooperative interactions between water and phosphate moieties and macrocyclic amine/ammonium groups that exhibit a certain level of preorganization but also some degree of conformational flexibility. This study has provided an opportunity to examine the variability in the hydrogen bonding modes of protonated forms of **L** and phosphate. It builds on the study by Bazzicalupi et al.,[6] where thermodynamic properties of adducts formed by macrocyclic polyamines and PO_4^{3-} and $P_2O_7^{4-}$ in solution were presented.

Experimental Section

Materials and Methods. Commercial reagents, purchased from Aldrich or BDH, were used as received. 1,4,7,10,13,16-Hexaazacyclooctadecane (**L**, [18]aneN$_6$) can be prepared by the classical Richman−Atkins synthesis.[23] In this work, it was collected as a byproduct of the 1,4,7-triazacyclonane synthesis.[23] Typically, 50.0 g of disodium-N,N′,N″-tris(*p*-tolysolfonyl)diethylenetriamine (0.08 mol) and 30.3 g of 1,2-bis(*p*-tolysulfonyloxy)-ethane (0.08 mol) were reacted in DMF. Following hydrolysis with sulfuric acid and treatment with concentrated HCl, tacn·HCl was collected and the volume of the filtrate was reduced to about $^1/_3$. Refrigeration of the solution for several days yielded a mixture of hydrosulfate and hydrochloride salts of **L** (1.08 g), which was collected and dissolved in distilled water (40 mL) containing NaOH (0.92 g). The solution was taken to dryness and 100 mL of toluene was added. Following azeotropic distillation to remove water, the mixture was filtered and the toluene solution was set aside. The procedure was repeated with a further 100 mL of toluene. The fractions were combined, reduced in volume to 100 mL, and cooled to room temperature, producing feathery needles of **L**, which were collected by filtration and air-dried to give a white solid (yield 0.46 g, 2.2%).

Physical Measurements. Infrared spectra were recorded on a Perkin-Elmer 1640 FTIR spectrometer. Microanalyses were performed by the Campbell Microanalytical Service, Dunedin, NZ.

Syntheses. (H$_6$L)(H$_2$PO$_4$)$_6$·2H$_3$PO$_4$ (1). The free ligand **L** (58 mg, 0.22 mmol) was dissolved in a small amount of water and phosphoric acid (concentrated, 218 mg). Slow evaporation of the aqueous solution gave colorless crystals of **1** that were suitable for single-crystal X-ray diffraction studies (yield of **1** = 138 mg, 59%). Microanalysis (%) found: C, 14.2; H, 5.2; N, 8.0. Calcd. for $C_{12}H_{54}N_6O_{32}P_8$: C, 13.8; H, 5.2; N, 8.1. Selected IR bands ν (KBr disk, cm^{-1}): 3414s, 3066s, 3028s, 2922s, 2855s, 2522m, 1637m, 1461m, 1122s, 1100s 1062s, 994s, 964s, 844m, 795m, 537m, 493s.

(H$_6$L)(H$_2$PO$_4$)$_6$ (2). A solution of **L** (57 mg, 0.22 mmol) and phosphoric acid (concentrated, 218 mg) was prepared as described for **1** and the pH was adjusted to 3 with 5 M NaOH. Slow evaporation gave a mixture of **1** and **2** that could be separated manually. Yield of **2** = 90 mg, 50%. Microanalysis (%) found: C, 16.7; H, 5.6; N, 9.4. Calcd. for $C_{12}H_{48}N_4O_{24}P_6$: C, 17.0; H, 5.7; N, 9.9. Selected IR bands ν (KBr disk, cm^{-1}): 3444m, 3337m, 3055s, 2791s, 2533m, 2422m, 1673m, 1622m, 1588m, 1500w, 1464m, 1449m, 1289m, 1233m, 1137s, 1040s, 955s, 891s, 794m, 751m, 537m, 496s.

(H$_4$L)(H$_2$PO$_4$)$_4$ (3). A solution of **L** (58 mg, 0.22 mmol) and phosphoric acid (concentrated, 218 mg) was prepared as described for **1** and the pH was adjusted to 6 with 1 M NaOH. Slow diffusion of ethanol into this solution yielded colorless crystals of **3** that were suitable for single-crystal X-ray diffraction studies; however separation of sufficient material for microanalysis from the cocrystallized sodium phosphate and **4** proved difficult. Yield of **3** ≈ 25 mg, 17%. Microanalysis (%) found: C, 11.7; H, 5.3; N, 6.5. Calcd. for $C_{12}H_{62}N_6Na_4O_{38}P_8$ (**3** with four NaH_2PO_4 and six H_2O): C, 11.6; H, 5.1; N, 6.5.

(H$_4$L)(H$_2$PO$_4$)$_4$·2H$_2$O (4). A solution of **L** (26 mg, 0.10 mmol) and phosphoric acid (concentrated, 300 mg) was prepared as described for **1** and the pH was adjusted to 6 with 5 M NaOH. Slow evaporation gave a mixture of **4** and NaH_2PO_4 that proved difficult to separate. Yield ≈ 30 mg, 20%. Microanalysis (%) found: C, 15.9; H, 5.7; N, 9.0. Calcd. for $C_{12}H_{50}N_6Na_2O_{26}P_6$ (**4** with two NaH_2PO_4): C, 15.6; H, 5.4; N, 9.1. Selected IR bands ν (KBr disk, cm^{-1}): 3424s, 3059s, 2855s, 2788s, 2433m, 1703m, 1655m, 1622m, 1588m, 1462m, 1405w, 1289m, 1233m, 1139s, 1056s, 940s, 894s, 794m, 750m, 496s.

(H$_4$L)(HPO$_4$)$_2$·7H$_2$O (5). A solution of **L** (67 mg, 0.26 mmol) and phosphoric acid (concentrated, 251 mg) was prepared as

(13) (a) Junk, P. C. *Rev. Inorg. Chem.* **2001**, *21*, 93. (b) Junk, P. C.; Smith, M. K.; Steed, J. W. *Polyhedron* **2001**, *20*, 2979.
(14) Brudenell, S. J.; Spiccia, L.; Hockless, D. C. R.; Tiekink, E. R. T. *J. Chem. Soc., Dalton Trans.*, **1999**, 1475.
(15) Smith, C. B.; Stevens, A. K. W.; Wallwork, K. S.; Lincoln, S. F.; Taylor, M. R.; Wainwright, K. P. *Inorg. Chem.* **2002**, *41*, 1093.
(16) Beer, P. D.; Cadman, J.; Lloris, J. M.; Martinez-Máñez, R.; Padilla, M. E.; Pardo, T., Smith, D. K.; Soto, J. *J. Chem. Soc., Dalton Trans.* **1999**, 127.
(17) Beer, P. D.; Cadman, J. *New. J. Chem.* **1999**, *23*, 347.
(18) Lee, C.; Lee, D. H.; Hong, J. *Tetrahedron Lett.* **2001**, *42*, 8665.
(19) Liao, J.; Chen, C.; Fang, J. *Org. Lett.* **2002**, *4*, 561.
(20) Bencini, A.; Bianchi, A.; Giorgi, C.; Paoletti, P.; Valtancoli, B. *Inorg. Chem.* **1996**, *35*, 1114.
(21) Bazzicalupi, C.; Bencini, A.; Bianchi, A.; Fusi, V.; Giorgi, C.; Granchi, A.; Paoletti, P.; Valtancoli, B. *J. Chem. Soc., Perkin Trans. 2* **1997**, 775.
(22) Kimura, E.; Kodama, M.; Yatsunami, T. *J. Am. Chem. Soc.* **1982**, *104*, 3182.
(23) Richman, J. E.; Atkins, T. J. *J. Am. Chem. Soc.* **1974**, *96*, 2268.

Table 1. Crystal and Refinement Data for **1**−**5**

identification code	**1**	**2**	**3**	**4**	**5**
empirical formula	$C_{12}H_{54}N_6O_{32}P_8$	$C_{12}H_{48}N_6O_{24}P_6$	$C_{21}H_{42}N_6O_{16}P_4$	$C_{12}H_{46}N_6O_{18}P_4$	$C_{24}H_{100}N_{12}O_{30}P_4$
fw	1042.38	846.38	650.40	686.42	1161.04
cryst syst	monoclinic	triclinic	monoclinic	monoclinic	triclinic
space group	P2(1)/n	$P\bar{1}$	P2(1)/n	P2(1)/n	$P\bar{1}$
a, Å	11.5267(2)	8.4826(1)	8.5026(2)	8.7901(3)	9.4687(1)
b, Å	14.1193(4)	8.8353(2)	13.4929(4)	16.1913(5)	10.3232(2)
c, Å	12.0357(3)	11.9115(3)	11.5923(3)	10.2531(4)	14.1338(3)
α, deg		105.894(1)			91.481(1)
β, deg	103.626(1)	105.484(1)	97.592(1)	98.324(2)	90.298(1)
γ, deg		97.444(1)			106.597(1)
vol, Å^3	1903.67(8)	807.41(3)	1318.27(6)	1443.88(9)	1323.43(4)
Z	2	1	2	2	1
ρ (calcd), gcm^{-3}	1.818	1.741	1.639	1.579	1.457
reflns collected	15944	9125	9492	9705	12429
independent reflns	4573	3938	3101	3538	6283
no. of parameters	343	310	256	267	516
GOF on F^2	0.966	1.03	1.006	0.934	1.032
R1, wR2 [$I > 2\sigma(I)$][a]	0.0431, 0.0921	0.0421, 0.0954	0.0411, 0.0806	0.0458, 0.0872	0.0384, 0.0912
R1, wR2 (all data)[a]	0.0814, 0.1036	0.0617, 0.1041	0.0740, 0.0888	0.1011, 0.1012	0.0539, 0.0990

[a] $R1 = \Sigma||F_0| - |F_c||/\Sigma|F_0|$; $wR2 = [\Sigma w(F_o^2 - F_c^2)^2/\Sigma w(F_o^2)^2]^{1/2}$.

described for **1** and the pH was adjusted to 8 with 5 M NaOH solution. Slow evaporation gave crystals of **5** that were suitable for single-crystal X-ray diffraction studies. Yield of **5**, 36 mg, 24%. Microanalysis (%) found: C, 24.8; H, 8.9; N, 14.2. Calc. For $C_{12}H_{50}N_6O_{15}P_2$: C, 24.8; H, 8.7; N, 14.5. Selected IR bands *ν* (KBr disk, cm^{-1}): 3421s, 3308s, 3088m, 2864m, 2788m, 2744m, 2611m, 2533m, 1627m, 1521m, 1481m, 1462m, 1227m, 1140m, 1066s, 1027s, 998s, 959s, 907m, 753m, 577m, 526s.

X-ray Crystallography. General Procedures. A summary of the crystal data and structure refinement for **1**−**5** is given in Table 1. Single-crystal X-ray data were collected on an Enraf-Nonius CAD4 diffractometer with monochromated Mo Kα radiation (λ = 0.71073 Å) at 123(2) K using phi and/or omega scans. Data were corrected for Lorentz and polarization effects and absorption corrections were applied. The structures were solved by the direct methods and refined using the full matrix least-squares method of the programs SHELXS-97[24] and SHELXL-97,[25] respectively. The program X-Seed[26] was used as an interface to the SHELX programs, and to prepare the figures. In each case all non-hydrogen atoms were refined anisotropically. In the figures, dashed lines represent hydrogen bonds and, where ORTEP representation has been used, ellipsoids have been drawn at the 50% probability level.

Specific Comments. (1) $(H_6L)(H_2PO_4)_6\cdot 2H_3PO_4$. The locations of the phosphate and phosphoric acid hydrogen atoms were deduced from interatomic distances and residual electron density, then restrained to idealized geometries. All C and N protons were located on final Fourier difference maps and refined isotropically.

(2) $(H_6L)(H_2PO_4)_6$. All hydrogen atoms were located on Fourier difference maps and refined isotropically except for H(4P) which became unstable during refinement. This proton, the location of which was inferred by residual electron density and the proximity of host oxygen, O(4P3), to that of a neighboring phosphate (O(4P3)-H(4P)···O(4P1) 2.502(2) Å, 174.7°) was introduced and refined at an idealized geometry.

(4) $(H_4L)(H_2PO_4)_4\cdot 2H_2O$. Two phosphate protons (H(2P) and H(3P)) were restrained to idealized geometries, deduced from residual electron density and the proximities of their respective H-bonds donor/acceptor oxygen atoms (O(4P2)-H(2P)···O(2P1) 2.609(3) Å, 167.2°, O(1P1)-H(3P)···O(1W) 2.589(2) Å, 152.6°). All other hydrogen atoms were located on final Fourier difference maps and refined isotropically.

(3) $(H_4L)(H_2PO_4)_4$ and (5) $(H_4L)(HPO_4)_2\cdot 7H_2O$. All OH and NH hydrogen atoms were refined isotropically and unrestrained after being located unambiguously on Fourier difference maps. Some C−H hydrogen atoms were modeled using idealized geometries.

Results and Discussion

Synthesis and Characterization. Four of the five macrocycle−oxoanion adducts reported herein crystallized on slow evaporation of aqueous solutions containing [18]aneN$_6$ (**L**) and phosphoric acid, and whose pH had been adjusted to one of four values in the 1−8 range, viz., $(H_6L)(H_2PO_4)_6\cdot 2H_3PO_4$ (**1**) at pH 1, $(H_6L)(H_2PO_4)_6$ (**2**) at pH 3, $(H_4L)(H_2PO_4)_4$ (**3**) and $(H_4L)(H_2PO_4)_4\cdot 2H_2O$ (**4**) at pH 6, and $(H_4L)(HPO_4)_2\cdot 7H_2O$ (**5**) at pH 8. We note, however, that a mixture of **2** and **3** was obtained at pH 3 and a mixture of **3** and **4** was obtained at pH 6, along with coprecipitation of sodium dihydrogen phosphate. The large crystals obtained at pH 8 (**5**) crystallized from a more dilute solution than the other adducts and therefore were easily obtained free of cocrystallized sodium dihydrogen phosphate. This product was surprisingly insoluble in water once formed. The IR spectra showed C−H, N−H, and O−H stretches in the expected regions and absorbances due to the phosphates in the 900−1200 cm^{-1} range.

Crystal Structure Determination. As a general note, the high quality of the crystals has allowed good quality data to be collected from which almost all hydrogen atoms could be located on Fourier difference maps during refinement. This assisted greatly in the evaluation of H-bonding contributions to the structural assemblies formed by the protonated [18]aneN$_6$ macrocycle in association with mono- and dihydrogen phosphate and, where present, phosphoric acid and water of crystallization. The $H_2PO_4^-$ anions are all characterized by two long (ca. 1.57 Å) and two short (ca. 1.51 Å) P−O bonds, the former corresponding to those of the

(24) Sheldrick, G. M. *SHELXS-97*; University of Göttingen, Germany, 1997.
(25) Sheldrick, G. M. *SHELXL-97*; University of Göttingen, Germany, 1997.
(26) Barbour, L. J. X-Seed-A software tool for supramolecular crystallography. *J. Supramol. Chem.* **2001**, *1*, 189.

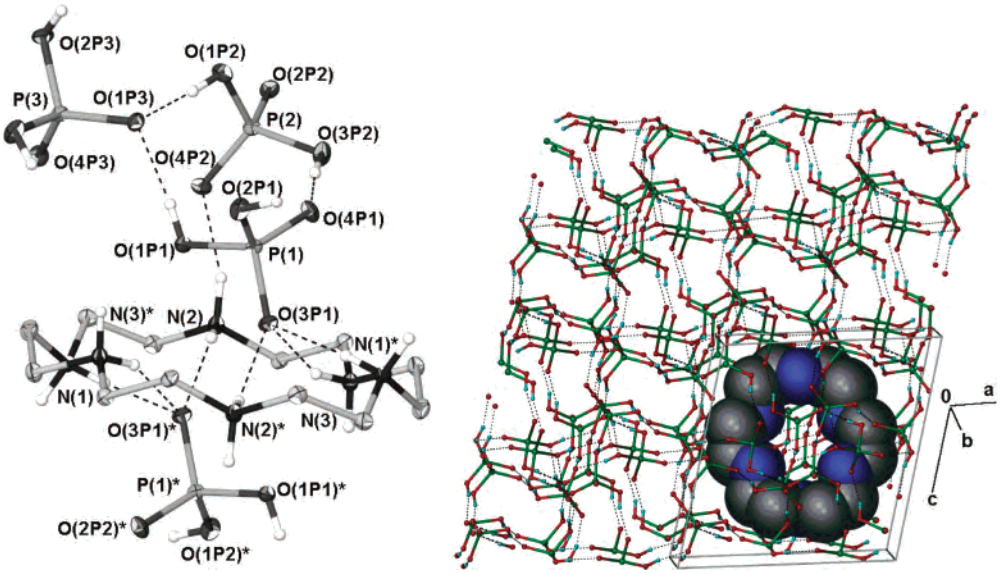

Figure 1. (a) ORTEP plot of [18]aneN$_6$ and phosphate anions in **1**. Phosphoric acid molecule and C−H hydrogen atoms omitted for clarity (left). (b) Packing of [18]aneN$_6$ in the 3D phosphate network in **1** showing one of four macrocycles as van der Waals spheres (right).

protonated oxygen atoms (Table 1). The HPO_4^{2-} anions have one long (ca. 1.57 Å), two intermediate (ca. 1.53 Å), and one short (ca. 1.51 Å) P−O bond, with the longer bond involving the protonated oxygen atom. In the few cases where the hydrogen atoms could not be located, these characteristics were used to identify the proton-bearing oxygen atoms.

$(H_6L)(H_2PO_4)_6\cdot 2H_3PO_4$ (1). The crystal structure of **1** consists of a fully protonated macrocycle, $[H_6L]^{6+}$, which is embedded in a highly interconnected 3-dimensional phosphate network formed by six dihydrogen phosphate counterions and two phosphoric acid solvent molecules. The macrocycle uses all 12 ammonium protons to H-bond to the eight phosphate moieties. Three dihydrogen phosphate anions form a bridge across the macrocycle both above and below the plane of the macrocycle. There are two symmetry-related $H_2PO_4^-$ anions bound on either side of the macrocycle via η-3 H-bonds to a single oxygen atom, O(3P1) (Figure 1a), a feature of all adducts except for **3**, where the cavity anions only have η-2 H-bonds to a single oxygen atom. The phosphoric acid molecule (P(4)) has a short O···O (O(1P4)···O(4P3)) distance to a neighboring phosphate anion (2.429(3) Å), indicating that proton H(9P) represented as being located on O(1P4), may have been shared between the two oxygen atoms (this proton became unstable during isotropic refinement). This proposal is difficult to defend as the best solution was found with a restrained, idealized geometry and attempts to model the proton with a range of partial occupancies gave larger final indices. The macrocycles are arranged in a herringbone pattern within the tightly packed phosphate network shown in Figure 1b. Recent discussions in the literature have highlighted the importance of C−H···X interactions in crystal packing.[27−29] Although the predominant interactions in the present structure are of the O−H···O and N−H···O types, there is one reasonably close C−H···O contact (C(4)−H(12)···O(4P4) 3.290(3) Å).

$(H_6L)(H_2PO_4)_6$ (2). In **2**, the hexaprotonated macrocycle lies around a crystallographic inversion center, and uses all of its ammonium protons to form hydrogen bonds to the $H_2PO_4^-$ anions (Figure 2a). Phosphate, P(3), accepts three H-bonds from three unique macrocyclic ammonium groups to one of its oxygen atoms and another from N(2)* to its other nonprotonated oxygen, O(2P3) (2.769(2) Å). O(2P3) is also bound to an ammonium group of an adjacent macrocycle. There is a further H-bond to one of the OH groups of this anion involving a macrocyclic C−H group as the donor (C(4)−H(6)···O(3P3) 3.267(3) Å), giving this $H_2PO_4^-$ anion the highest number of contacts with the macrocycle of any of the phosphate moieties in this series. This adduct and also **3** are different from **1**, **4**, and **5** in that the cavity phosphates in the latter interact with protons on the host macrocycle via one oxygen atom only. The other two dihydrogen phosphate anions in **2** are involved solely in O−H···O hydrogen bonding with the exception of one weak C−H···O contact for the P(2) phosphate (C(2)−H(10)···O(2P2) 3.343(2) Å) and one N−H···O contact for the P(1) phosphate (N(1)−H(1A)···O(1P1) 2.802(2) Å). The macrocycles in **2** form stacks parallel to the *b* axis and lie closer together than those in **1** being bridged by one oxygen (N(2)···O(3P2)···N(3)*) whereas in the other structure the shortest inter-macrocyclic bridge is across a phosphate anion (N···O−P−O···N). The 3D phosphate network surrounding the macrocycles in **2** is not as complex or tightly packed as that found in **1** (Figure 2b).

$(H_4L)(H_2PO_4)_4$ (3). The structure of **3** consists of the tetraprotonated macrocycle, which utilizes all eight ammonium protons to bind four $H_2PO_4^-$ anions (two above and two below the plane of the ring). It is the only one in the series not to exhibit the η-3 macrocyclic H-bonding mode seen in the other structures (Figure 3a). **3** is most closely related to **4** in composition but lacks the inclusion of solvent

(27) Desiraju, G. R. *Acc. Chem. Res.* **1996**, *29*, 441.
(28) Cotton, F. A.; Daniels, L. M.; Jordan, G. T., IV; Murillo, C. A. *J. Chem. Soc., Chem. Commun.* **1997**, 1673.
(29) Mascal, M. *J. Chem. Soc., Chem. Commun.* **1998**, 303.

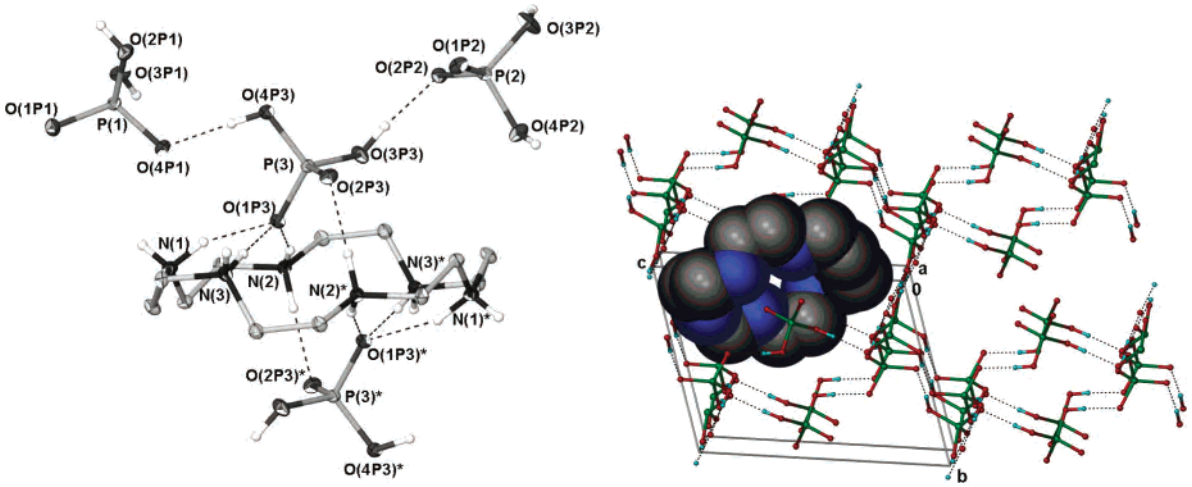

Figure 2. (a) ORTEP plot of [18]aneN$_6$ and dihydrogen phosphate anions in **2**. C−H hydrogens and some symmetry-related anions below macrocyclic ring omitted for clarity (left). (b) Packing of [18]aneN$_6$ in 3D phosphate network in **2** showing one macrocycle as van der Waals spheres (right).

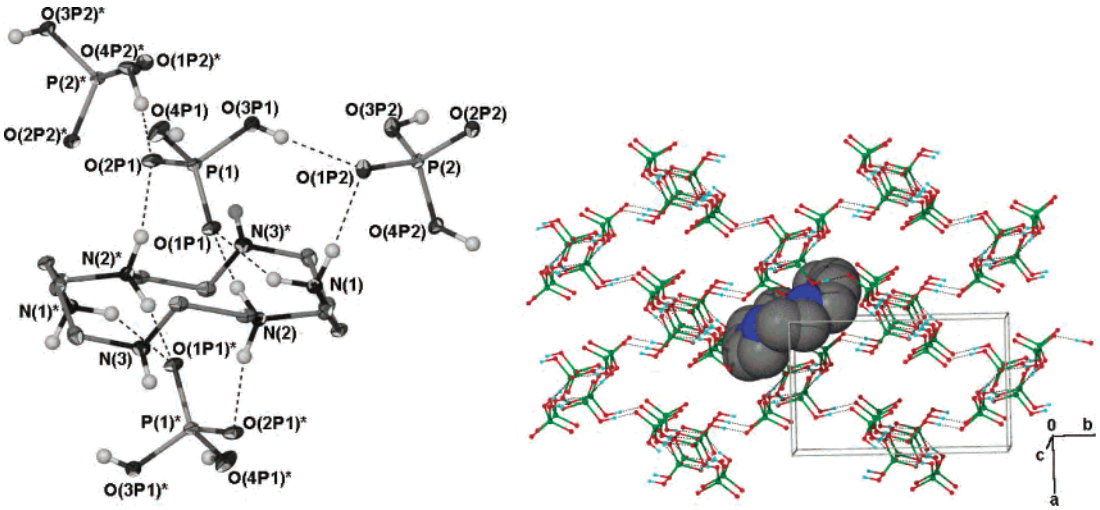

Figure 3. (a) ORTEP plot of [18]aneN$_6$ and phosphate anions in **3**. C−H hydrogens and some symmetry-related anions below the ring have been omitted for clarity (left). (b) Packing of [18]aneN$_6$ in the 3D phosphate network in **3** showing one macrocycle as van der Waals spheres (right).

waters. The anions form a three-dimensional network via a complex hydrogen bonding scheme that houses the macrocycles (Figure 3b), which are separated by 3.67 Å (C(6) − C(6)*). One short C−H···O interaction was found involving the macrocycle and one of the phosphate oxygen atoms (C(3)−H(8)···O(3P2), 3.272(3) Å), which, as in the case of one like contact in **2**, also hosts a proton. The two $H_2PO_4^-$ anions are participating in six (P(1)) and five (P(2)) H-bonding interactions. The P(1) anion lies within the macrocyclic cavity and one of its nonprotonated oxygen atoms interacts with two ammonium groups, N(1) and N(2), and the other accepting two H-bonds: one from the symmetry related N(2) of the same macrocycle and another from an OH group (O(4P2)) on the other $H_2PO_4^-$ anion. The other anion is hydrogen bonded top-to-tail with a symmetry related P(2) phosphate that is reminiscent of carboxylic acid H-bond pairs (O(3P2)-H(3P)···O(2P2)). The macrocycles form stacks similar to those found in **2** but these stacks are not as perfectly aligned.

$(H_4L)(H_2PO_4)_4\cdot 2H_2O$ (4). In **4**, one of the adducts obtained at pH 6, the charge on each tetraprotonated macrocycle is balanced by four dihydrogen phosphate anions (two unique).

A water molecule acts as a hydrogen bond donor bridging between symmetry related phosphates (P(2) and P(2)*) and as an acceptor from O(1P1). The macrocycle exhibits η-3 N−H···O interactions to symmetry related phosphate oxygens (N(1), N(2), and N(1)* to O(4P1): 2.755(3) Å, 2.945(3) Å, and 2.869(3) Å, respectively) above and below the ring, albeit via a different arrangement from those found in **1** and **2** owing to the presence of the two amines (N(3) and N(3)*) that interact weakly with O(3P2)* and O(3P2), respectively (3.113(3) Å). The dihydrogen phosphate anions interact in a top-to-tail fashion, as described for **3**, to generate a 3D H-bonded network that encases that macrocycle (Figure 4). Despite the included water molecule being the only compositional difference between the present structure and **3**, there is a significant rearrangement of the lattice and H-bonding pattern. Although the 3D network formed by the phosphate and water molecules is similar to that found in **2**, the macrocycles pack in a more pronounced herringbone pattern and adopt a different conformation.

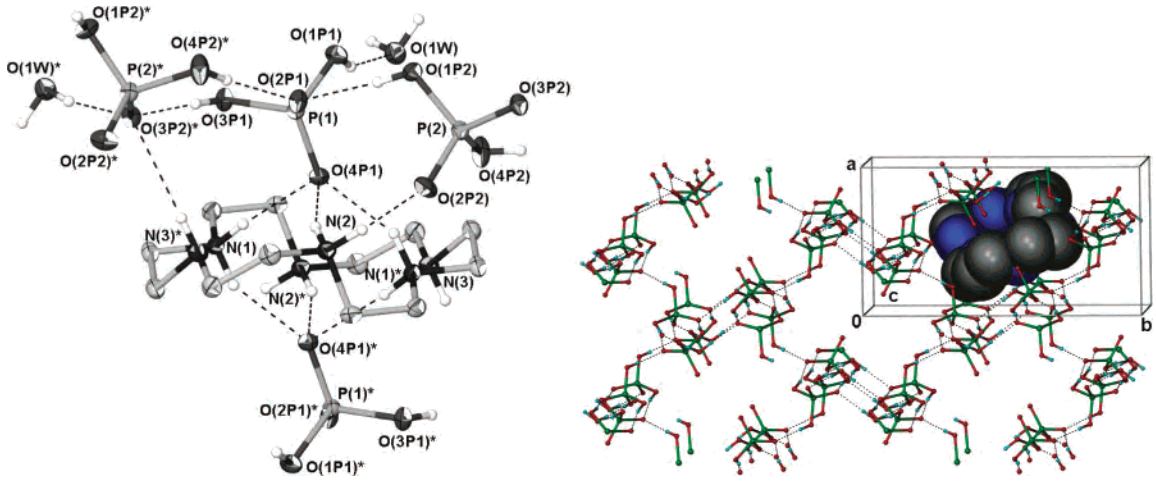

Figure 4. (a) ORTEP plot of [18]aneN$_6$ and phosphate anions in **4**. C−H hydrogens and some symmetry-related anions below the ring omitted for clarity (left). (b) Packing of [18]aneN$_6$ in the 3D phosphate network in **4** showing one macrocycle as van der Waals spheres (right).

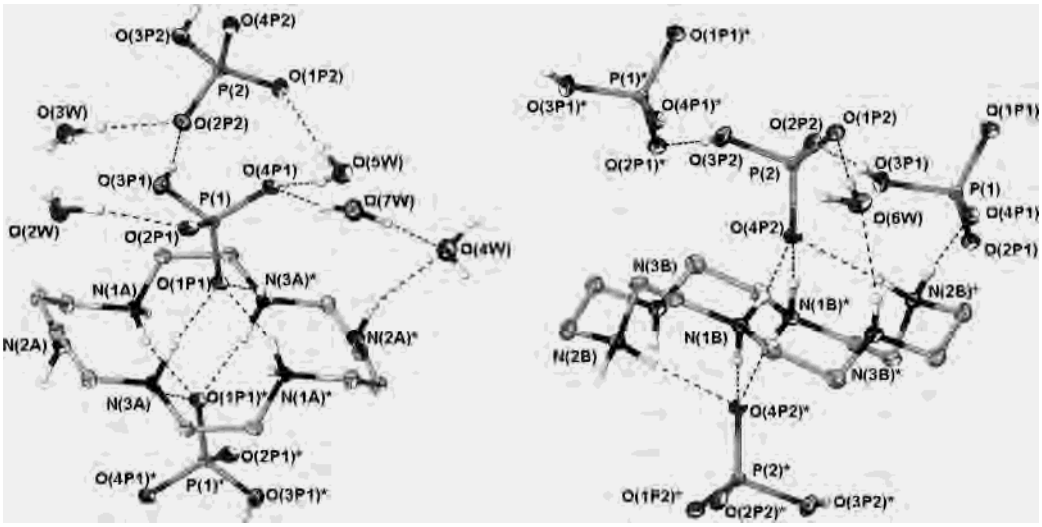

Figure 5. ORTEP plot of the macrocycles (A and B, left and right, respectively), hydrogen phosphate anions, and selected water molecules in **5**. C−H hydrogens and some symmetry-related anions below the ring omitted for clarity.

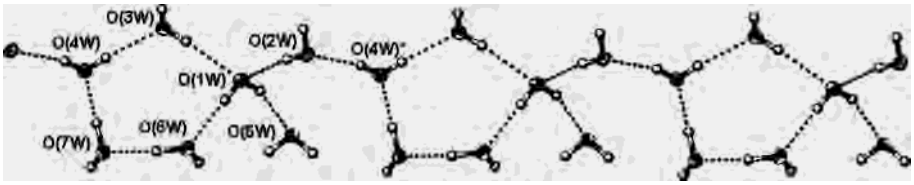

Figure 6. ORTEP plot of the water chain in **5** (* indicates symmetry generated atom).

$(H_4L)(HPO_4)_2.7H_2O$ (5). The structure formed at pH 8 (adduct **5**) is the most complex of the series in terms of hydrogen bonding and supramolecular interactions. The ionic component consists of two crystallographically unique macrocycles (A and B) and four hydrogen phosphate anions (Figure 5). Both macrocycles are tetraprotonated with the now-familiar η-3 H-bonding to a phosphate oxygen (O(1P1) for macrocycle A and O(4P2) for macrocycle B) as seen in other structures reported here. Macrocycle B differs from A only in that its amines hydrogen bond to symmetry related water molecules, O(6W) and O(6W)* (N(3B)-H(5)···O(6W) 2.9255(18) Å), whereas the amines in macrocycle A at best have very weak interactions with O(4W) and O(4W)* (3.367(2) Å).

The water molecules occupy the channels formed by the 2-dimensional sheets of macrocycle and phosphate, forming a chain with a string-of-pearls motif comprised of a cyclic pentamer with one dangling water molecule and another bridging to the next pentamer to form a linear sequence of repeating heptamers (Figure 6). Each water molecule uses both hydrogen atoms in H-bonding. Two of the water molecules (O(1W) and O(4W)) form H-bonds only to other water molecules, another (O(5W)) is a H-bond donor to oxygens on two HPO_4^{2-} anions and the other four form H-bonds to both a water and a HPO_4^{2-} anion. Two water molecules found in the structure act as double-donor/double-acceptor waters (O(1W) and O(6W)) with the rest acting as double donors to water and/or phosphate oxygen atoms and

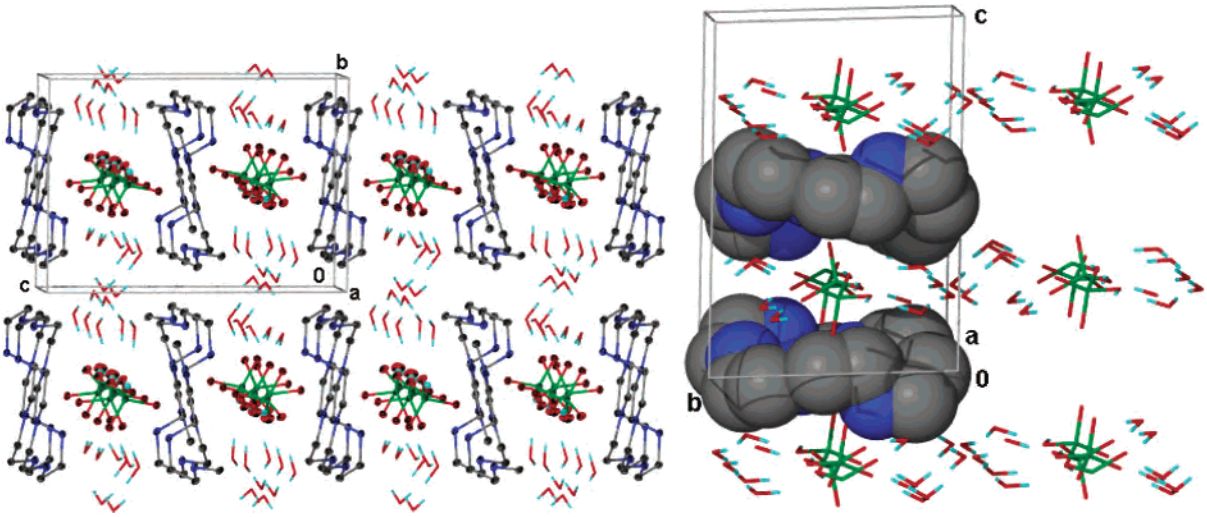

Figure 7. (a) Packing of macrocycles and phosphates (ORTEP) and water molecules (stick) viewed down the water channels (left). (b) Packing of [18]-aneN$_6$ in the 3D phosphate network in **5**, with each crystallographically unique macrocycle A and B shown as van der Waals spheres for clarity (right).

single acceptors from other water molecules. There is a slight lengthening of the H-bonds along the shortest path of the chain, O(2)−O(1)−O(3)−O(4)−O(2)*, where the strain would be if the water chain had tensile force exerted upon it. The average O···O distance is 2.91 Å, whereas along the longer pathway, O(2)−O(1)−O(6)−O(7)−O(4)−O(2)*, the average is 2.79 Å. The cyclic pentamer is quite distorted from a regular five-membered ring (102°), with O−O−O angles varying from 85.8 to 131.1° and the small O−O−O−O torsion angles (1.5 to 9.7°) indicate that the ring is nearly planar. Two structures incorporating water heptamers have been previously reported[30,31] and, notably, a string-of-pearls motif is found in the structure reported by Foces-Foces et al.,[30] but is comprised of six- rather than the five-membered water rings of **5**.

The monohydrogen phosphate anions are more heavily involved in hydrogen bonding than their mono-negative conjugate acid in the previous structures. Both unique anions are involved in η-3 coordination motif with three ammonium groups (from macrocycle A for P(1) and macrocycle B for P(2)) to one nonprotonated oxygen atom. Another oxygen atom on each anion is accepting H-bonds from two water molecules and an ammonium group on an adjacent macrocycle, and their third nonprotonated oxygen atom accepts H-bonds from a water molecule and a hydroxyl function from the other anion. The waters and anions connect through a complex array of hydrogen bonds to form 2D sheets between which the macrocycles lie (Figure 7).

Degree of Protonation and Conformation of [18]aneN$_6$. As noted above, in every structure the macrocycle lies around a crystallographic inversion center. The observation that in the adducts formed at pH 6 and 8 the macrocycles are tetraprotonated ($[H_4L]^{4+}$) is unexpected, given that in aqueous solution deprotonation of $[H_4L]^{4+}$ to give $[H_3L]^{3+}$ occurs at much lower pH (*viz.*, pK_{a3} for $[H_6L]^{6+}$ = 4.1).[32] Consequently, a very small proportion of the tetraprotonated macrocycle (<2%) will be present in solution at pH ≥ 6. Similarly, the crystallization of the fully protonated macrocycle, $[H_6L]^{6+}$, in adduct **2**, isolated at pH 3, is unexpected given that pK_{a1} and pK_{a2} for $[H_6L]^{6+}$ (both < 2) indicate that the tetraprotonated state, $[H_4L]^{4+}$ should be predominant. Since the degree of protonation of the macrocycle is higher in the crystallized adduct than the average protonation level in solution, crystallization will lead to an increase in solution pH. Through a combination of interactions the anions and solvent of crystallization provide an environment within which particular protonated forms of the macrocycle can crystallize even at pH values outside their normal regions of stability.

To present time, literature contains no structurally characterized examples of $[H_5L]^{5+}$ or $[H_3L]^{3+}$ and only one of $[H_2L]^{2+}$,[33] however there are occurrences of $[H_4L]^{4+}$ [6,34,35] and $[H_6L]^{6+}$ adducts.[36,37] This is an interesting observation given that potentiometric studies have provided evidence for the formation of 1:1 adducts of $[H_5L]^{5+}$ with $H_2PO_4^-$ and $[H_3L]^{3+}$ with both $H_2PO_4^-$ and HPO_4^{2-}. It appears that the protonated macrocycles with a symmetric arrangement of ammonium ions crystallize more readily from solution. Due to the requirement for charge neutrality 1:1 adducts could not be isolated in the solid state. Introduction of weakly interacting anions as cocrystallization agents could allow this. In the two macrocycle-pyrophosphate structures reported by Bazzicaluppi et al.,[6] 2:1 anion ($H_2P_2O_7^{2-}$) to macrocycle

(30) Foces-Foces, C.; Cano, F. H.; Martinez-Ripoll, M.; Faure, R.; Roussel, C.; Claramunt, R. M.; López, C.; Sans, D.; Elguero, J. *Tetrahedron: Asymmetry* **1990**, *1*, 65.
(31) Van Langenberg, K.; Batten, S. R.; Berry, K. J.; Hockless, D. C. R.; Moubaraki, B.; Murray, K. S. *Inorg. Chem.* **1997**, *36*, 5006.
(32) Kimura, E.; Koike, T. *J. Chem. Soc., Chem. Commun.* **1998**, 1495.
(33) Zhou, P.; Xue, F.; Au-yeng, S. C. F.; Xu, X.-P. *Acta Crystallogr., Sect. B: Struct. Sci.* **1999**, *55*, 389.
(34) Cullinane, J.; Gelb, R. I.; Margulis, T. N.; Zompa, L. J. *J. Am. Chem. Soc.* **1982**, *104*, 3048.
(35) Thuéry, P.; Keller, N.; Lance, M.; Vigner, J.-D.; Nierlich, M. *Acta Crystallogr., Sect. C: Cryst. Struct. Commun.* **1995**, *51*, 1407.
(36) Wardem, A. C.; Warren, M.; Hearn, M. T. W.; Spiccia, L. *New J. Chem.* **2004**, 1160.
(37) Margulis, T. N.; Zompa, L. J. *J. Heterocycl. Chem.* **1983**, *20*, 975.
(38) Margulis, T. N.; Zompa, J. L. *Acta Crystallogr., Sect. B: Struct. Crystallogr. Cryst. Chem.* **1981**, 37, 1426.

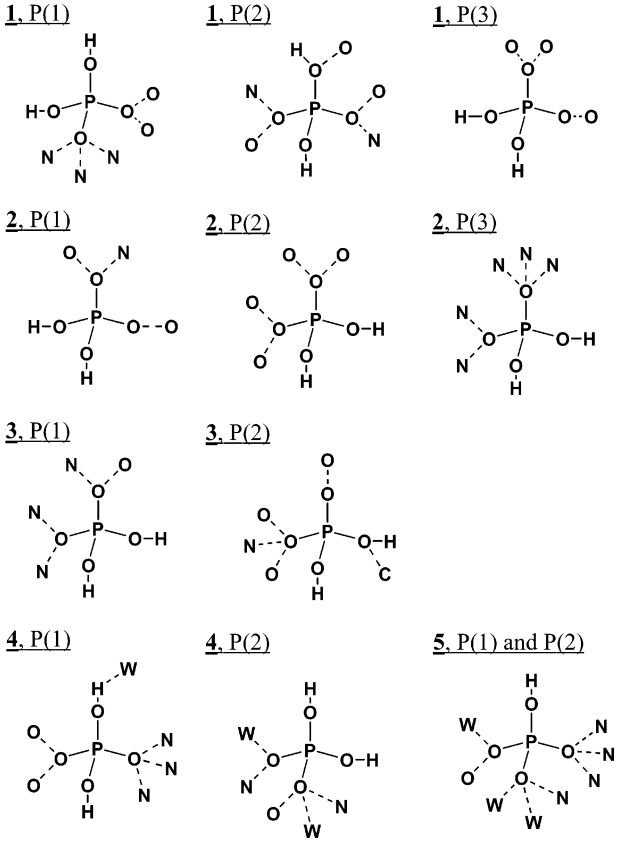

Figure 8. H-bonding modes for the phosphate anions and phosphoric acid found in **1**−**5**. Dashed lines represent H-bonds accepted by phosphates (O = phosphate oxygen, N = ammonium, W = water, C = carbon). All phosphate OH groups donate to a phosphate oxygen unless otherwise indicated.

($[H_4L]^{4+}$) adducts crystallize for solutions containing a 1:1 mixture of reagents.

In terms of the conformations of the macrocycle, there is no apparent correlation between degree of protonation and conformational preference for [18]aneN_6, indicating that intramacrocyclic charge−charge repulsion forces have a smaller influence on conformation than H-bonding effects and crystal packing forces. There is considerable variation in the conformation of the tetraprotonated macrocyle ($[H_4L]^{4+}$) in **2**−**5** and the conformation in **1** ($[H_6L]^{6+}$) is much closer to that found in **3** than all others.

Phosphate Binding Sites. The structures reveal a high degree of variability in donor/acceptor distribution across the phosphate anions. Figure 8 shows the different H-bonding modes for phosphate anions found in **1**−**5**. All of the phosphate groups in question use all their hydroxyl protons to donate to phosphate or water. In one case, a P−OH oxygen also accepts a hydrogen bond from another phosphate anion (O(2P3)−H(2P3)···O(1P2) 2.732(3) Å in **1**) and there is an instance of a phosphate hydroxyl oxygen accepting a C−H hydrogen bond (C(3)−H(8)···O(3P2) 3.272(3) in **3**). The possible hydrogen bonding interactions between the macrocycle and either the phosphates or water molecules are as follows:

-N−H^+···$^-$O-	(1.1)
-N−H^+···OH-	(1.2)
-N−H···$^-$O-	(1.3)
-N−H···OH-	(1.4)
-O−H···:NH	(1.5)
-C−H···$^-$O	(2.1)
-C−H···OH-	(2.2)

The vast majority of the interactions are of type 1.1 as may have been anticipated given the combination of strong electrostatic interactions and H-bonding effects. An example of a type 1.3 interaction was found in **3** (N(3)−H(3A)···O(3P2)#1, 3.113(3)). This particular interaction is found in an adduct formed at pH 6, where one would mainly expect to find interactions of type 1.1 and 1.2. Type 1.3 hydrogen bonds appear unable to induce complex formation in solution,[6] but are facilitated by charge separation across the $H_2PO_4^-$ anion in the solid state, induced by dipole−dipole and charge−dipole interactions. There are two N−H···O(W) H-bonds (type 1.4) between macrocyclic amines and water molecules in **4** (N(2A)−H(8)···O(4W)#5 3.367(2) Å and N(3B)−H(5)···O(6W)#3 2.9240(18) Å). Surprisingly, no instances of type 1.2 interactions were found in the series, even at very low pH values.

Conclusion

Conjugate bases of phosphoric acid form adducts with the heaxaazamacrocycle, [18]aneN_6, the composition of which varies with the pH of crystallization. Tetra- and hexaprotonated forms of the macrocycle are able to switch between two general conformations (flat or condensed), which provide sufficient spatial flexibility to accommodate the various populations of phosphate oxoanions and water molecules that combine to form 2D and 3D arrays in the solid state. The phosphate moieties are able to accept one to three hydrogen bonds to their nonprotonated oxygen atoms and, in some cases, one to their hydroxyl oxygen atom(s). At higher pH, the incorporation of water aids in the formation of stable structures.

Acknowledgment. This work was supported by the Australian Research Council. A.C.W. was the recipient of a Research Fellowship and Departmental Scholarship from Monash University.

Supporting Information Available: H-bonding parameters and crystallographic data in CIF format for **1**−**5**. This material is available free of charge via the Internet at http://pubs.acs.org.

IC049633V